Virology 423 (2012) 152–164

Contents lists available at SciVerse ScienceDirect

Virology

journal homepage: www.elsevier.com/locate/yviro

CD4- and dynamin-dependent endocytosis of HIV-1 into plasmacytoid dendritic cells

Kathrin Pritschet [a], Norbert Donhauser [a], Philipp Schuster [a], Moritz Ries [a], Sabrina Haupt [a], Nicolai A. Kittan [a], Klaus Korn [a], Stefan Pöhlmann [b], Gudrun Holland [c], Norbert Bannert [c], Elke Bogner [d,1], Barbara Schmidt [a,*,1]

[a] Institute of Clinical and Molecular Virology, National Reference Centre for Retroviruses, Friedrich-Alexander-Universität Erlangen-Nürnberg, 91054 Erlangen, Germany
[b] Institute of Virology, Hannover Medical School, 30625 Hannover, Germany
[c] Robert Koch-Institute, Center for Biological Security 4, 13353 Berlin, Germany
[d] Institute of Virology, Charité University Hospital, 10117 Berlin, Germany

ARTICLE INFO

Article history:
Received 2 August 2011
Accepted 29 November 2011
Available online 29 December 2011

Keywords:
Dendritic cell
HIV
Immunopathogenesis
Entry
Interferon, type I

ABSTRACT

Chronic immune activation, triggered by plasmacytoid dendritic cell (PDC) interferon (IFN)-alpha production, plays an important role in HIV-1 pathogenesis. As the entry of HIV-1 seems to be important for the activation of PDC, we directly characterized the viral entry into these cells using immuno-electron microscopy, cellular fractionation, confocal imaging, and functional experiments. After attachment to PDC, viruses were taken up in an energy-dependent manner. The virions were located in compartments positive for caveolin; early endosomal antigen 1; Rab GTPases 5, 7 and 9; lysosomal-associated membrane protein 1. PDC harbored more virus in endocytic vesicles than CD4+ T cells ($p<0.05$). Blocking CD4 inhibited the uptake of virions into cytosolic and endosomal compartments. Dynasore, an inhibitor of dynamin-dependent endocytosis, not the fusion inhibitor T-20, reduced the HIV-1 induced IFN-alpha production. Altogether, our morphological and functional data support the role of endocytosis for the entry and IFN-alpha induction of HIV-1 in PDC.

Introduction

Chronic immune stimulation with high T cell turnover rates and apoptosis has been identified as a major hallmark of pathogenic lentiviral infection (Kirchhoff, 2009). In HIV-1 infected patients, the degree of immune stimulation is more closely associated with progression to AIDS than viral load (Giorgi et al., 1999; Sousa et al., 2002). An important stimulus triggering immune activation is the type I interferon (IFN) production, which drives a potent Th1 polarization (Cella et al., 2000). The IFN-alpha induction by (non)-infectious HIV-1 particles enhances the expression of the TNF-related apoptosis-inducing ligand (TRAIL) and its death receptor (DR) 5 on CD4+ T lymphocytes in the peripheral blood and in secondary lymphatic tissue (Herbeuval et al., 2005b, 2006), resulting in the apoptosis of uninfected CD4+ bystander T cells which correlates with progression to disease (Herbeuval et al., 2005a). In primate lentiviral models, pathogenic SIV infections have also been associated with increased IFN-alpha and TRAIL levels (Mandl et al., 2008; Meythaler et al., 2009).

In 1999, plasmacytoid dendritic cells (PDC) were identified as major producers of type I IFN in the blood (Cella et al., 1999; Siegal et al., 1999). These cells, although accounting for only 0.2–0.5% of peripheral blood mononuclear cells (PBMC), play an important role in innate immune defenses against bacterial and viral pathogens (Fitzgerald-Bocarsly and Feng, 2007). PDC express the endosomal Toll-like receptors (TLR) 7 and 9, which, after detection of single-stranded RNA and CpG-like DNA molecules, respectively, initiate a downstream signaling cascade resulting in the transcription of proinflammatory cytokines and interferons (Gilliet et al., 2008). These soluble factors orchestrate the early immune response via stimulation of naïve T cells, thus linking innate and adaptive immunity (Kadowaki et al., 2000).

High-titered HIV-1 and HIV-infected cells induce major IFN-alpha production by PDC (Beignon et al., 2005; Fong et al., 2002; Fonteneau et al., 2004; Herbeuval et al., 2005a, 2005b; Schmidt et al., 2005; Yonezawa et al., 2003). The underlying mechanism for the PDC activation involves the interaction of the HIV-1 envelope protein gp120 with the CD4 receptor on PDC, supported by the finding that the affinity of gp120 to CD4 determines the degree of IFN-alpha production (Haupt et al., 2008). The HIV-1 coreceptors CXCR4 and CCR5 appear to play a role in the productive infection of PDC (Schmidt et al., 2004), but are dispensable for IFN-alpha induction (Beignon et al., 2005; Haupt et al., 2008; Herbeuval et al., 2005b; Schmidt et al., 2005). The IFN-alpha production is not affected by fusion inhibitors, but can be blocked by lysosomotropic drugs such as chloroquin, bafilomycin, and ammonium chloride, which provide indirect evidence for the uptake of HIV-1 by endocytosis (Beignon et al., 2005; Hardy et al., 2007; Schmidt et al., 2005). Recombinant virions deficient in viral RNA packaging were profoundly impaired in IFN-alpha induction, suggesting viral nucleic acids interact with TLR 7 as stimulatory component (Beignon et al., 2005). A recent study confirmed the role of TLR 7 and suggested cytoplasmic receptors as additional sensors for HIV-infected cells (Lepelley et al., 2011).

* Corresponding author. Fax: +49 9131 85 26485.
E-mail address: baschmid@viro.med.uni-erlangen.de (B. Schmidt).
[1] Contributed equally to the work.

0042-6822/$ – see front matter © 2011 Elsevier Inc. All rights reserved.
doi:10.1016/j.virol.2011.11.026

The major endocytic pathways are clathrin- and caveolar/raft-mediated endocytosis, macropinocytosis and phagocytosis. Further mechanisms have emerged, but are less well characterized. Clathrin- and caveolin-mediated endocytosis can be identified by their respective vesicle coat protein. Both entry mechanisms are dependent on the cytosolic GTPase dynamin that promotes pinching off the primary endocytic vesicles from the plasma membrane. Once internalized, viruses are routed to early endosomes, which contain the Rab GTPase 5 and the early endosomal antigen 1 (EEA-1) (Mu et al., 1995; Rubino et al., 2000). The trafficking pathway continues towards late endosomes, characterized by the Rab proteins 7 and 9, and lysosomes in which the lysosomal-associated membrane protein 1 (LAMP-1) is highly enriched. Moreover viral particles can be recycled to the cell surface in CD71-positive vesicles (Di Pucchio et al., 2008). Tetraspanins like CD63 and CD81 have also been reported to play a role in the pathogenesis of HIV-1 in CD4+ T cells and antigen-presenting cells. In this respect, tetraspanin microdomains may facilitate HIV-1 binding by clustering the receptor CD4 or the coreceptors (Martin et al., 2005; Mercer et al., 2010; Schelhaas, 2010; van Spriel and Figdor, 2010).

The entry of HIV-1 into PDC has so far only been assessed by indirect methods, namely the effect of inhibitors of the endosomal acidification on the HIV-1 induced IFN-alpha production. In our current study, we aimed to directly visualize and further characterize the uptake mechanism using immuno-electron microscopy, cellular fractionation, and confocal imaging. These approaches together with the analysis of different entry inhibitors on the IFN-alpha production provided morphological and functional evidence for a CD4- and dynamin-dependent uptake of HIV-1 into PDC. This entry mechanism, which appears to be a major factor in the HIV-1 immunopathogenesis, may represent a new therapeutic target for AIDS and its related disorders.

Results

Attachment and uptake of viral particles into PDC

IFN-alpha induction by HIV-1 and HIV-infected cells can be inhibited by blocking endosomal acidification (Beignon et al., 2005; Hardy et al., 2007; Martinson et al., 2010; Schmidt et al., 2005), providing indirect evidence for the endocytosis of viral particles. To directly visualize this process, we analyzed the entry of the X4-tropic primary isolate HIV-1_{SF33} and the molecular clone HIV-1_{NL4-3} into PDC using transmission electron microscopy in combination with pre- and post-embedding immunostaining. The images presented are taken from a series of 11 independent experiments. HIV-1 attached to the dendrites of PDC (Fig. 1A), confirmed by staining with anti-p24 and a Gold-conjugated IgG (Fig. 1B). Gold-covered particles were also detected in intracellular vesicles of PDC (Fig. 1C). When HIV-exposed PDC were stained with the secondary reagent only, Gold particles were absent from the preparation. Instead, the characteristic morphology of HIV-1 particles was revealed in more detail (Fig. 1D), most notably the conical capsids (Fig. 1E). Serial thin section series of virus-containing vesicles, which were obtained from single cells, suggested that most of the vesicles were indeed intracellular and not just invaginations of the plasma membrane (data not shown). When the energy-dependent entry of HIV-1 was blocked at 4 °C, viral particles still attached to the PDC, however, uptake was only observed at 37 °C (data not shown). These data suggest that viral particles, after attachment to PDC, are taken up into vesicular compartments of these cells.

Presence of HIV-1 in intracellular compartments of PDC

After entry of HIV-1 into PDC, viral capsids were detected in close proximity to (Fig. 2A) or within vesicular structures of these cells (Fig. 2B). Some particles appeared to be attached to the vesicular membrane (Fig. 2C), whereas others were free-floating in this compartment (Fig. 2D). Immunolabeled HIV-1 particles were surrounded by electron-lucent material, which did only marginally stain with anti-p24 (Fig. 2D). The specificity of staining was confirmed in neutralization experiments, in which the p24 antibody was preincubated with a tenfold excess of p24 antigen (Aalto Bio Reagents Ltd., Dublin, Ireland). This procedure largely reduced the detection signals in 293T cells transfected with pNL4-3 in immunofluorescence (Fig. S1A), and in immuno-electron microscopy (Fig. 1C, Fig. S1B). Unspecific staining of the p24 antibody was not observed, using PDC not exposed to HIV-1_{SF33} (data not shown). Altogether, the images support the presence of virions in intracellular vesicles of PDC.

Enhanced uptake of HIV-1 particles into endosomes of PDC

In a next step, we performed cellular fractionation experiments to study the distribution of HIV-1 RNA in cytosolic and vesicular compartments of CD4+ T cells and PDC. To confirm that vesicles were effectively separated from the cytosol, Western blot analyses were performed using an antibody to LAMP-1, which is tightly associated with vesicular membranes. LAMP-1 was mostly detected in the vesicular fraction, whereas only a faint band was observed in the cytosolic extract, similarly observed for CD4+ T cells and PDC (Fig. 3A). First, we analyzed the kinetics of the HIV-1 uptake into CD4+ T cells and PDC. The HIV-1 RNA increased in both cell populations from 15 to 120 min of incubation, with a more rapid and efficient uptake into PDC (Fig. 3B). After 45 min, PDC harbored four times more viral RNA in endosomal vesicles than CD4+ T cells ($36{,}141 \pm 10{,}343$ copies/ml versus $7{,}953 \pm 1{,}308$ copies/ml; $p = 0.003$), determined in 6 and 12 separate experiments, respectively. This difference was still significant for the percentage of HIV-1 RNA in the endosomal fraction of PDC compared to CD4+ T cells (74.1% versus 52.8%, respectively, $p = 0.03$) (Fig. 3C). Thus, PDC appear to have an increased capacity to endocytose HIV-1 in comparison to CD4+ T cells.

Role of endocytosis and fusion for the uptake of HIV-1

The extent of fusion and endocytosis for the uptake of HIV-1 into PDC and CD4+ T cells was analyzed at different inhibitory conditions. The energy-dependent processes of fusion and endocytosis can be blocked at 4 °C. Consequently, incubation on ice reduced the HIV-1 RNA in cytosolic and vesicular compartments of PDC and CD4+ T cells by at least 70% (Fig. 3D). A neutralizing antibody to CD4 (Leu3a) decreased the viral uptake by more than 75% in CD4+ T cells and to a minor extent in PDC; viral RNA was reduced in vesicular and cytosolic compartments of CD4+ T cells and in the vesicular fraction of PDC (Fig. 3E). Additionally we evaluated the effect of T-20, a small C-peptide that prevents fusion of HIV-1 with the cellular membrane by binding to the transmembrane glycoprotein gp41 and inhibiting the 6-helix bundle formation (Kilby et al., 1998). T-20 blocked the HIV-1 infection of an indicator cell line ($p < 0.05$) (data not shown). The abundance of HIV-1 RNA in cellular fractionation experiments, however, was only marginally reduced in CD4+ T cells and PDC at concentrations of 100 nM and higher (Fig. 3F and data not shown). In CD4+ T cells, HIV-1 RNA decreased in the cytosol and increased in the vesicles, whereas in PDC, HIV-1 RNA rather declined in the vesicular fraction. Altogether, inhibitory conditions revealed comparable HIV-1 RNA changes in PDC and CD4+ T cells, supporting a similar route of entry in both cell populations.

Dynasore reduces the HIV-1 mediated IFN-alpha induction

To determine further the role of fusion and endocytosis for the uptake of HIV-1 into PDC, we investigated the effects of T-20 and dynasore on the IFN-alpha production. Dynasore is a small molecule that inhibits the cytosolic GTPase dynamin and thereby blocks clathrin- and caveolin-mediated endocytosis (Macia et al., 2006). PDC were

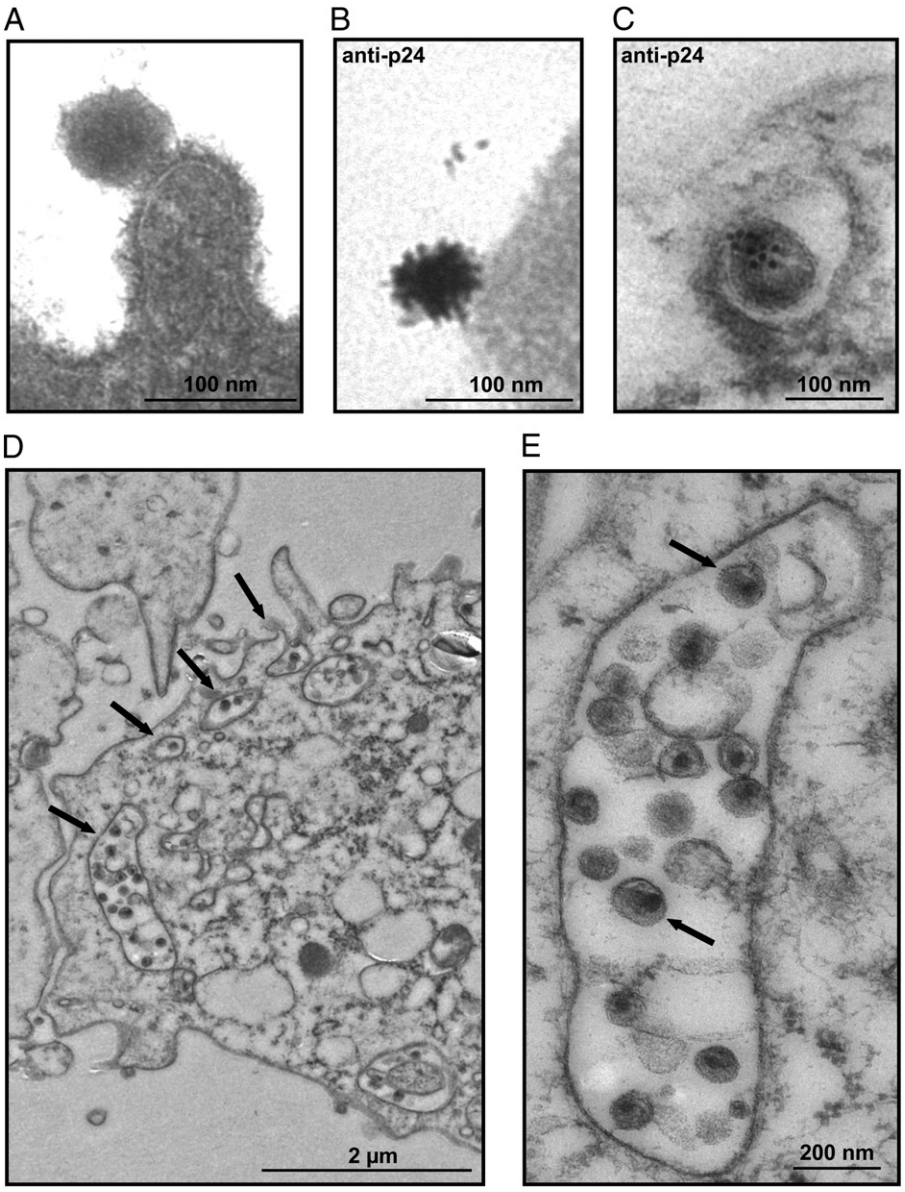

Fig. 1. Attachment and entry of HIV-1 into plasmacytoid dendritic cells (PDC). (A) Transmission electron microscopy and (B–E) immunostaining of PDC exposed to the X4-tropic primary isolate HIV-1_{SF33} or the molecular clone HIV-1_{NL4-3}. Figures were either taken from (B) pre-embedding or (C–E) post-embedding immunostaining, using (B, C) a monoclonal antibody to p24 antigen (anti-p24) and a Gold-conjugated anti-human immunoglobulin or (D, E) the secondary reagent only. Arrows point to (D) the uptake of viral particles into vesicular structures of PDC, and, in more detail, (E) the characteristic morphology of HIV-1 particles. Images are taken from a series of 11 independent experiments using PDC of different donors.

pretreated with T-20 or dynasore for 30 min at 37 °C and then exposed to HIV-1_{NL4-3} for 36 h. T-20 neither affected the HIV-1 nor the HSV-1 induced IFN-alpha production (Fig. 4A), suggesting that fusion is not relevant for IFN-alpha induction. On the contrary, dynasore significantly reduced the IFN-alpha induction by HIV-1 to 22.6% in ten separate experiments ($p<0.001$) (Fig. 4B). In comparison, the IFN-alpha production in response to the TLR 7 agonist S-27609 was only reduced to 47.13% ($p<0.001$). According to previous studies (Carter et al., 2011), we investigated the effect of dynasore on the PDC activation in the absence of FCS. The effect of the inhibitor was more pronounced using these conditions. A toxic effect of dynasore or DMSO on the PDC was excluded by Annexin and propidium iodide staining after 36 h of incubation (Fig. 4C). Moreover, we investigated the effect of dynasore on the expression of CD4 and the coreceptors CXCR4 and CCR5 on the PDC. CD4 and CCR5 were not and CXCR4 slightly but not significantly downregulated within 2 h of incubation, which is considered to be the relevant time frame for the entry of HIV-1 (Fig. 4D). In addition, we directly studied the effect of dynasore on the uptake of HIV-1 into endosomal compartments of PDC using confocal imaging. Dynasore considerably reduced the colocalization of the viral capsid protein p24 with the early endosomal antigen 1 (EEA-1) at 15 min of incubation, and with the lysosomal-associated membrane protein 1 (LAMP-1) at 120 min of incubation (Fig. 4E). Thus, our findings suggest that a dynamin-dependent entry mechanism is involved in the internalization of HIV-1 and subsequent IFN-alpha induction in PDC rather than direct fusion of the virus with the plasma membrane.

HIV-1 is targeted to endosomal organelles

To characterize the uptake of HIV-1 into PDC in more detail, we performed confocal imaging using established markers of endocytic compartments, including EEA-1 as early and LAMP-1 as late endosomal marker. PDC were exposed to HIV-1_{SF33} or HIV-1_{NL4-3} for different time periods and then stained with antibodies against the viral capsid antigen p24 and EEA-1 or LAMP-1. When PDC were kept on ice during the entire incubation period, only very few red-stained

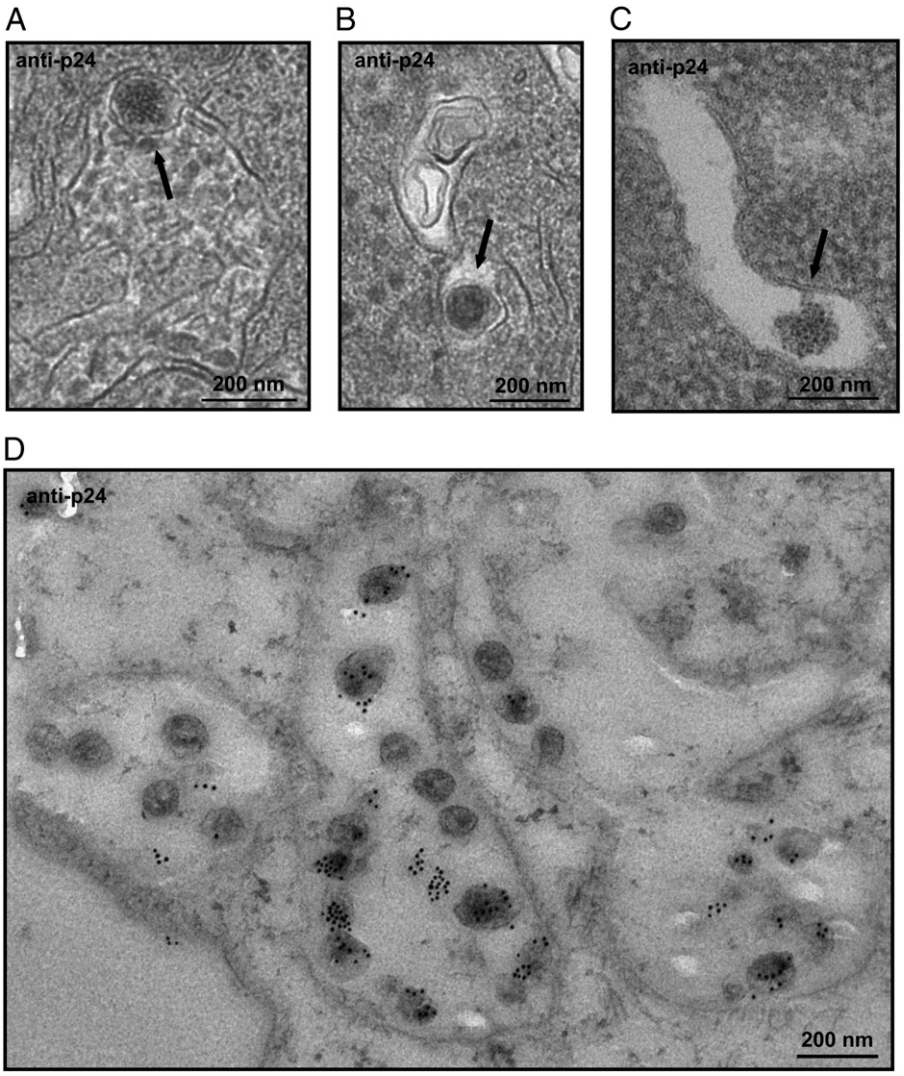

Fig. 2. Intracellular localization of HIV-1 in plasmacytoid dendritic cells (PDC). Immuno-electron microscopy of PDC exposed to the X4-tropic primary isolate HIV-1_{SF33} or the molecular clone HIV-1_{NL4-3}, using a monoclonal antibody to the capsid antigen p24 (anti-p24) and a Gold-conjugated anti-human immunoglobulin. The images were taken from (A-C) pre-embedding and (D) post-embedding immunostaining. Arrows point to single viral particles, which reside close to or within vesicular structures of PDC.

virions were detected, indicating that most particles at the cell surface were removed by the extensive washing procedure (Fig. 5A). Subsequent incubation of PDC at 37 °C showed colocalization of HIV-1 with EEA-1 within 15 min, indicative of rapid uptake into early endosomes (Fig. 5A). Notably, the extent of colocalization with EEA-1 at 15 min of incubation (57.41 ± 22.04%) was very similar to data recently published by others (O'Brien et al., 2011). The colocalization of EEA-1 with p24 antigen gradually decreased from 15 min to 120 min of incubation, which proved to be significant in statistical trend analysis ($p = 0.02$). In contrast, colocalization of p24 antigen with LAMP-1 significantly increased during this time period ($p < 0.001$) (Fig. 5B). This dynamics indicates that internalized virions are rapidly targeted to early endosomal compartments and subsequently transferred to late endosomes/lysosomes, providing evidence for endocytosis as a relevant entry route of HIV-1 into PDC. The three-dimensional aspect of the colocalization is illustrated by representative movies, which were obtained from EEA-1 and LAMP-1 Z-stacks using the Leica Visualization 3D-Projection program (Suppl. Figs. 2 and 3).

Intracellular trafficking of HIV-1 captured by PDC

To further characterize the compartments in which HIV-1 accumulates in PDC after internalization, we stained for early, maturating, and late endosomes (Rab GTPases 5, 7 and 9) (Mercer et al., 2010; Schelhaas, 2010), tetraspanins (CD81 and CD63) (van Spriel and Figdor, 2010), and recycling endosomes (CD71) (Di Pucchio et al., 2008). The amount of colocalization between HIV-1 and these cellular markers was quantified over time. On average, HIV-1 colocalized with the Rab GTPases in one third of the cells (Fig. 6A). Colocalization with Rab5 increased from 19% (30 min) to 31% (90 min) of incubation and decreased thereafter, whereas Rab7 and Rab9 signals slightly increased and did not decline within 120 min of incubation (Fig. S4A). The tetraspanins showed a strong colocalization for CD81 (37%) and to a lesser extent for CD63 (23%), whereas less than 7% of the viral capsids overlapped with the transferrin receptor CD71 (Fig. 6B). Colocalization with CD81 and CD63 occurred within 5–60 min of incubation (Fig. S4B). In conclusion, HIV-1 is rapidly taken up into endosomal compartments positive for CD81, CD63, and Rab GTPases. In contrast, viral capsids appear not to accumulate in CD71-positive vesicles indicating that HIV-1 is not shuttled back to the cell surface.

Internalization of HIV-1 particles through a Caveolin-1 mediated endocytic pathway

To verify that viral particles are internalized by a dynamin-dependent pathway, PDC were exposed to HIV-1_{NL4-3} as described above, this time

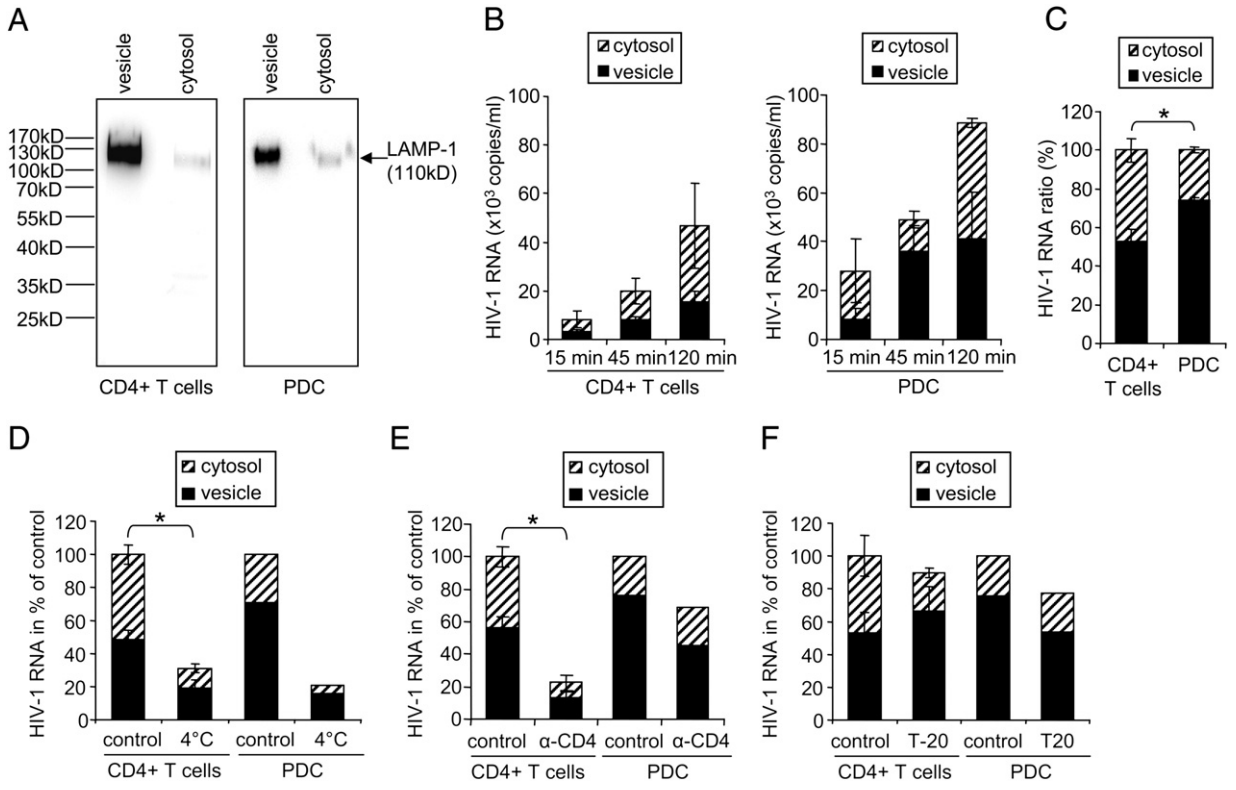

Fig. 3. Distribution of HIV-1 RNA in cytosolic and vesicular compartments of CD4+ T cells and plasmacytoid dendritic cells (PDC). (A) Western Blot analysis of cytosolic and vesicular fractions of CD4+ T cells and PDC exposed to HIV-1_{SF33}, using a monoclonal antibody against the lysosomal-associated membrane antigen 1 (LAMP-1). (B) Time course analysis of the uptake and cellular distribution of HIV-1 RNA in CD4+ T cells and PDC. The abundance of HIV-1 RNA is shown as mean and standard error of 6–12 separate experiments for CD4+ T cells, and 3, 6 and 4 separate experiments for PDC exposed to HIV-1 for 15, 45 and 120 min, respectively. (C) Distribution of HIV-1 RNA in cytosolic and vesicular compartments of CD4+ T cells and PDC, representative of 12 and 6 separate analyses, respectively. For each experiment, the HIV-1 RNA in both fractions was set to 100% (HIV-1 RNA ratio), calculating the proportion of HIV-1 RNA in each fraction. (D–F) Changes in HIV-1 RNA in different cell fractions after exposure of CD4+ T cells and PDC to HIV-1_{SF33} using (D) incubation at 4 °C, (E) a monoclonal antibody to CD4 (15 μg/ml), or (E) the fusion inhibitor T-20 (100 nM). The HIV-1 RNA in the uninhibited control sample was set to 100%. The results of CD4+ T cells are presented as mean and standard error of 3–4 separate experiments, the PDC data as mean of two separate experiments for each condition. Statistics were performed using the Student's t-test for independent and correlated samples, respectively. *$p<0.05$.

stained for clathrin and caveolin-1. On average, only 7% of the viral particles colocalized with the marker protein for clathrin-mediated endocytosis, whereas 37% overlapped with caveolin-1, a marker protein for the uptake by caveolae ($p=0.02$) (Fig. 7A). Colocalization of p24 antigen with caveolin-1 was observed within 5 min of incubation, whereas costaining with clathrin did not increase within 90 min of incubation. As a control, we investigated the colocalization of the transferrin receptor CD71 with clathrin, because transferrin is known to be taken up by clathrin-mediated endocytosis (Ehrlich et al., 2004; Hanover et al., 1984). CD71 rapidly and efficiently colocalized with clathrin within 5 min of incubation (Fig. 7A). These results, along with the reduction of IFN-alpha production by dynasore known to inhibit clathrin- and caveolin-mediated endocytosis, indicate that HIV-1 enters PDC at least in part through a caveolin- and dynamin-dependent pathway prior to inducing IFN-alpha.

Role of the CD4 receptor in the entry of HIV-1 into PDC

CD4 is well-known as receptor for the envelope-mediated fusion of HIV-1 with the cellular membrane. To investigate whether this receptor is also required for the endocytosis of HIV-1 into PDC, blocking experiments were performed. PDC were preincubated with a neutralizing antibody to CD4 (Leu3a) or human IgG as an isotype control at 37 °C for 2 h, and then exposed to HIV-1_{NL4-3} for 45 min at 37 °C. Thereafter, cells were labeled with antibodies against the viral capsid protein p24 and EEA-1. Confocal microscopy revealed that anti-CD4 inhibited the uptake of viral particles into cytosolic and endosomal compartments of PDC (Fig. 7B). In contrast, viral particles were readily taken up in both compartments in the presence of the isotype control and in mock-treated PDC. Additionally, we studied the effect of an antibody to BDCA2, a calcium-dependent lectin on the PDC surface, which mediates antigen capture and uptake (Dzionek et al., 2001) and binds to gp120 (Martinelli et al., 2007). Neither this antibody nor its isotype control blocked the internalization of HIV-1 into PDC (Fig. 7B). These results emphasize the crucial role of CD4 for the uptake and internalization of HIV-1 into cytosolic and endosomal compartments of PDC.

Discussion

The entry of HIV-1 into PDC has been addressed by several groups, providing indirect evidence that endocytosis of virions is required for the IFN-alpha induction (Fitzgerald-Bocarsly and Jacobs, 2010). Our study attempted to directly visualize the entry of the X4-tropic primary isolate HIV-1_{SF33} or the molecular clone HIV-1_{NL4-3} into freshly isolated PDC of healthy donors and elucidate some of the cellular factors required for successful entry and IFN-alpha induction by HIV-1 in PDC. In a first step, we focused on two-dimensional immuno-electron microscopy, which permitted us, for the first time, to directly visualize the presence of virions in intracellular vesicles of PDC (Figs. 1, 2). We observed Gold-covered viral capsids in vesicular structures of PDC in several pre- and post-embedding approaches in conjunction with control experiments. However, it has to be considered that this method has its limitations, as the cellular architecture is not completely illustrated (Bennett et al., 2009). Although three-dimensional reconstruction indicated that most of the vesicles were indeed intracellular, we cannot entirely exclude deep invaginations of the plasma membrane. Notably, the data obtained by electron microscopy were supported by confocal imaging,

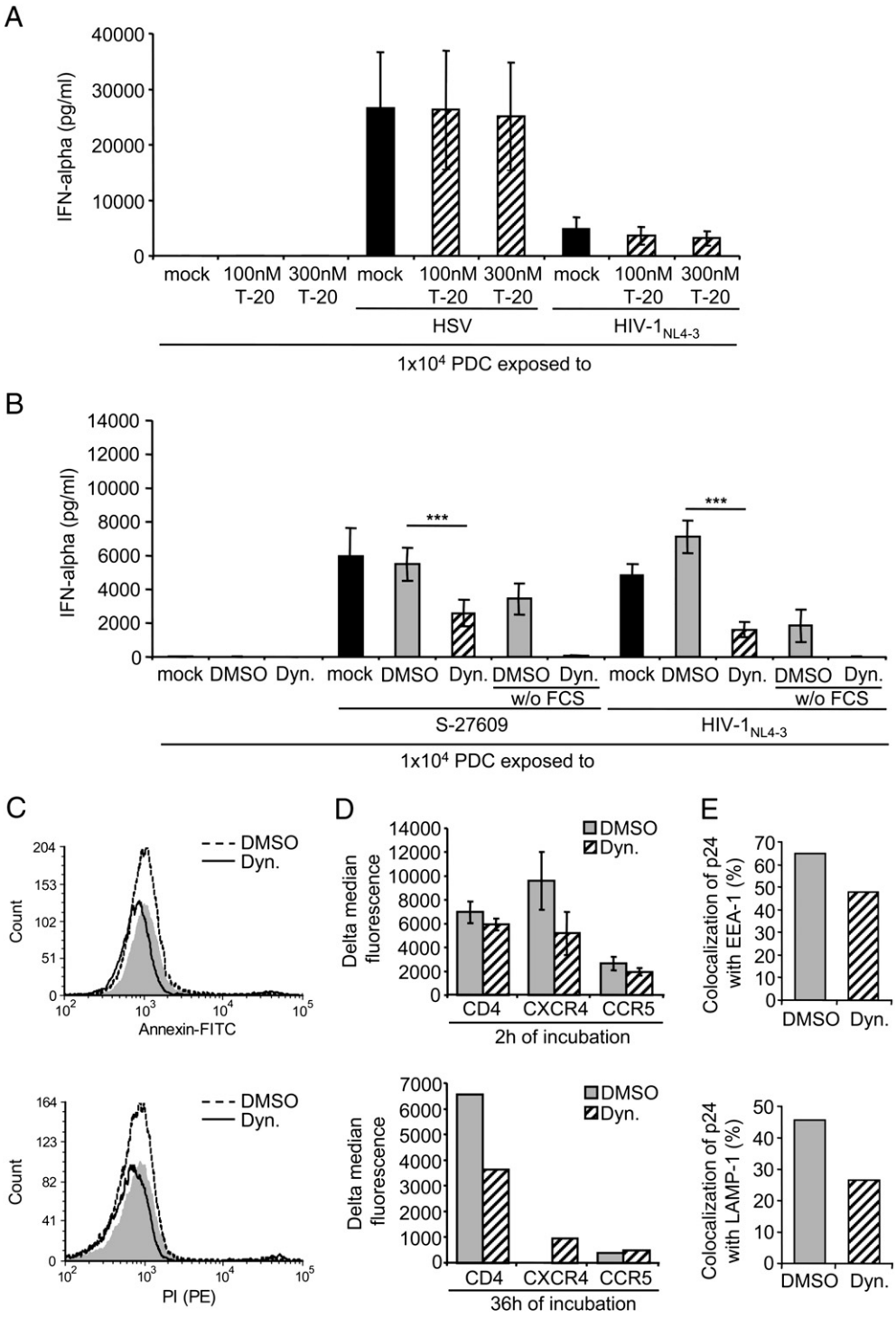

Fig. 4. Effect of T-20 and dynasore on the HIV-1 induced interferon (IFN)-alpha release by plasmacytoid dendritic cells (PDC). PDC were exposed to (A) the fusion inhibitor T-20 (100–300 nM) or (B) dynasore (Dyn.) (80 μM), an inhibitor of the GTPase dynamin, for 30 min and then stimulated with HIV-1_{NL4-3}. UV-irradiated herpes simplex virus type 1 (HSV-1) and the synthetic TLR 7 agonist S-27609 (5 μM) were used as control stimuli. Supernatants were harvested after 36 h and the IFN-alpha levels were determined by ELISA. Results are given as mean and standard error, representing ten separate experiments using PDC from different donors. In three experiments, PDC were incubated with dynasore and HIV-1 in the absence of fetal calf serum (w/o FCS) for 2 h. ***$p<0.001$. (C) Annexin and propidium iodide (PI) staining of PDC exposed to mock (grey filled curve), DMSO (dotted line) and dynasore (black line) for 36 h. (D) Expression of CD4 and the coreceptors CXCR4 and CCR5 on the PDC after 2 h and 36 h of incubation with DMSO or dynasore. Data are representative of three and two different donors, respectively. (E) Effect of dynasore on the colocalization of the viral p24 antigen with the early endosomal antigen 1 (EEA-1) or the lysosomal-associated membrane protein 1 (LAMP-1). Data are representative of 296 and 236 double-positive cells, respectively, using PDC of two different donors.

showing colocalization of viral capsids with several endosomal markers, including EEA-1, Rab GTPases, LAMP-1, and tetraspanins CD63 and CD81 (Fig. 5, Suppl. Figs. 2 and 3, Fig. 6). Altogether, our data support the presence of HIV-1 in endosomes, further corroborated by the results obtained by cellular fractionation (Fig. 3). Colocalization of HIV-1 with EEA-1 was similarly reported by others (O'Brien et al., 2011). In contrast to our data, they also reported costaining with CD71, but not with LAMP-1. These discrepancies may be due to methodological differences like different cell-culture conditions. While we used a primary HIV-1 isolate and a full-length proviral clone and stained with an antibody to p24 antigen,

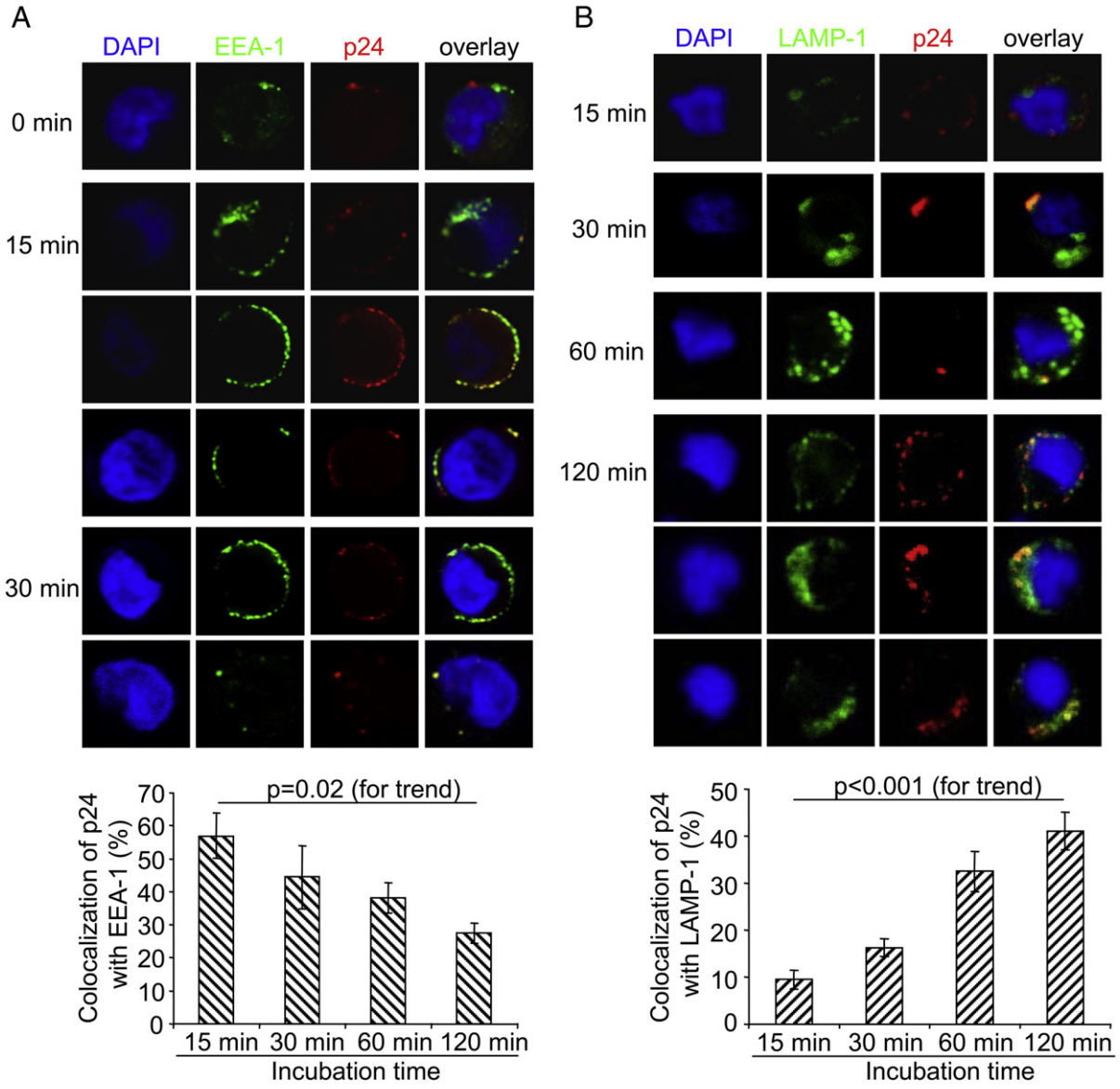

Fig. 5. Uptake of HIV-1 particles into early endosomes and lysosomes of plasmacytoid dendritic cells (PDC). PDC were exposed to the X4-tropic primary isolate HIV-1_{SF33} or HIV-1_{NL4-3} at 4 °C for 30–60 min and then incubated at 37 °C for different time periods. Cells were stained using a biotinylated antibody to the viral p24 capsid antigen (red) and a monoclonal antibody (green) against (A) the early endosomal antigen 1 (EEA-1) or (B) the lysosomal-associated membrane protein 1 (LAMP-1). Cell nuclei were stained with DAPI (blue). For quantification, double-positive cells were counted and the proportion of cells with a colocalization event was calculated. Data represent seven independent confocal experiments for EEA-1, evaluating a total of 162, 182, 109, and 113 double-positive cells for 15–20–60–120 min, and five separate experiments for LAMP-1, evaluating 255, 182, 278, and 227 double-positive cells for 15–30–60–120 min. Data are given as mean and standard error. Statistical analysis was performed using one way analysis of variance for trend analysis.

O'Brien and colleagues used GFP-HIV generated using a Vpr mutant and eGFP-Vpr plasmids (O'Brien et al., 2011).

Entry of HIV-1 can occur as CD4- and coreceptor-dependent fusion with the cellular membrane and as CD4-mediated, but coreceptor-independent endocytosis. The latter has been reported for primary CD4+ T cells (Blanco et al., 2004), and dynamin- and clathrin-mediated endocytosis for CD4+ HeLa cells (Daecke et al., 2005). Macropinocytosis was described as entry mechanism for HIV-1 into macrophages (Marechal et al., 2001), and further pathways have been addressed (Permanyer et al., 2010). To address the role of fusion and endocytosis for the uptake of HIV-1 into PDC and CD4+ T cells, we performed cellular fractionation experiments. Although we have to consider the relatively high background of the HIV-1 RNA, our data suggest a similar route of HIV-1 entry into PDC and CD4+ T cells. However, PDC harbored more HIV-1 RNA in endosomes than CD4+ T cells and thus have an increased capacity of endocytosis (Figs. 3B, C). Notably, the colocalization with different endosomal markers supports the conclusion that a substantial proportion of the HIV-1 particles are taken up into PDC via endocytosis (Figs. 6, 7A). Moreover, the fusion inhibitor T-20 did not substantially reduce the abundance of HIV-1 RNA in CD4+ T cells and PDC (Fig. 3F), which is consistent with a recent report that viral particles do not fuse at the plasma but the endosomal membrane (Miyauchi et al., 2009). It has to be considered that these results reflect our experimental conditions, in particular the high viral input, which was required to visualize the particles. Therefore, the uptake of HIV-1 into PDC may differ under more physiological conditions. The entry via endocytosis, however, may be favorable for HIV-1 because antibodies or entry inhibitors like T-20 do not readily gain access to this compartment.

In addition, we adopted a functional approach evaluating the effect of T-20 or dynasore on the HIV-1 induced IFN-alpha production. IFN-alpha induction was not affected by the fusion inhibitor T-20, but was sensitive to dynasore (Fig. 4), which prevents the dynamin-

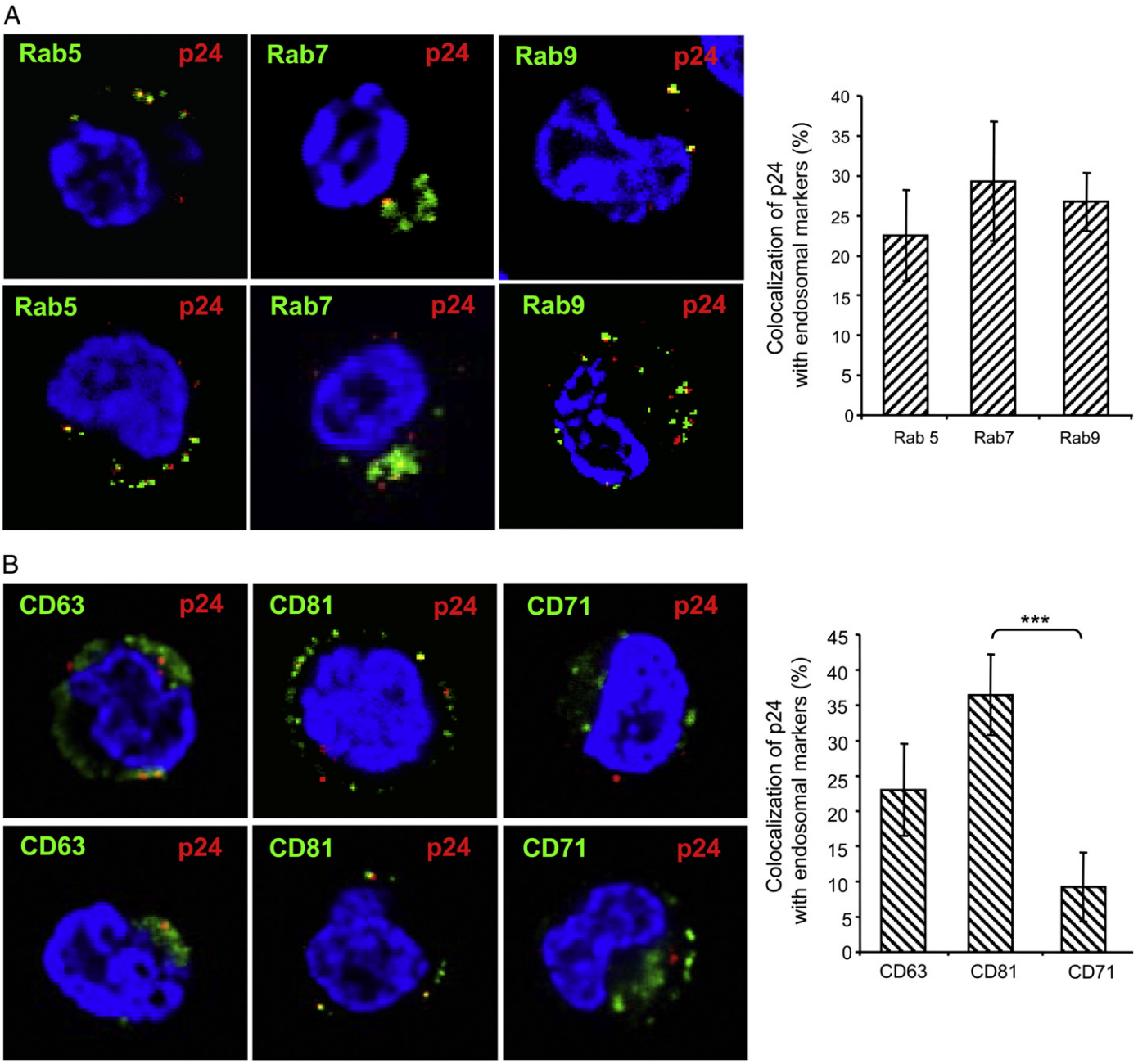

Fig. 6. Intracellular trafficking of HIV-1 captured by plasmacytoid dendritic cells (PDC). PDC were exposed to HIV-1_{NL4-3} at 4 °C for 30 min and then incubated at 37 °C for different time periods. Cells were labeled using a biotinylated antibody to the viral p24 capsid antigen (red), and monoclonal antibodies (green) to (A) the Rab GTPases 5, 7, and 9, (B) the tetraspanins CD63 and CD81, and the marker protein for recycling endosomes, CD71. Cell nuclei were stained using DAPI (blue). For quantification, double-positive cells were counted and the proportion of cells with a colocalization event was calculated. Data represent three independent confocal experiments, evaluating a total of 366, 412, and 304 double-positive cells for Rab5/7/9, and 368, 197 and 192 double-positive cells for CD63, CD81 or CD71. Data summarize all time points and are given as mean and standard error. Details are provided in Fig. S2. ***$p<0.001$.

dependent scission of clathrin- and caveolin-coated pits from the plasma membrane (Macia et al., 2006). A role of dynamin was also recently reported for the entry of HIV-1 into macrophages (Carter et al., 2011). Similarly, our data argue in favor of a dynamin-dependent uptake of HIV-1 into PDC to induce IFN-alpha production. As dynasore did not abolish IFN-alpha production completely, dynamin-independent pathways should also be considered. For instance, the role of autophagy-dependent viral recognition by PDC has been recently described (Lee et al., 2007). However, the signal for the autophagy marker LC3B was rather marginal, when we analyzed PDC with a respective antibody in confocal microscopy (data not shown).

Our confocal studies revealed that virions were internalized in caveolin-1 positive compartments (Fig. 7A). This was unexpected as caveolin-containing vesicles are reported to be much smaller (50–80 nm in diameter) than the relatively large HIV-loaded vesicles in the electron microscopy. However, endocytic vesicles appear to accommodate to their cargo, and several vesicles can merge into multivesicular bodies. Although clathrin-mediated endocytosis plays an important role for the entry of HIV-1 into several cell types (Permanyer et al., 2010), only a minority of particles colocalized with clathrin in our studies. However, these data are consistent, as clathrin colocalized with the transferrin receptor CD71, whereas neither of these markers costained with p24 antigen. Therefore, clathrin-mediated endocytosis of HIV-1 into PDC appears to be unlikely. Beyond that, other ways of endocytosis should be considered, which may also involve uptake of caveolin as part of the lipid rafts. In this respect, a recent study provided

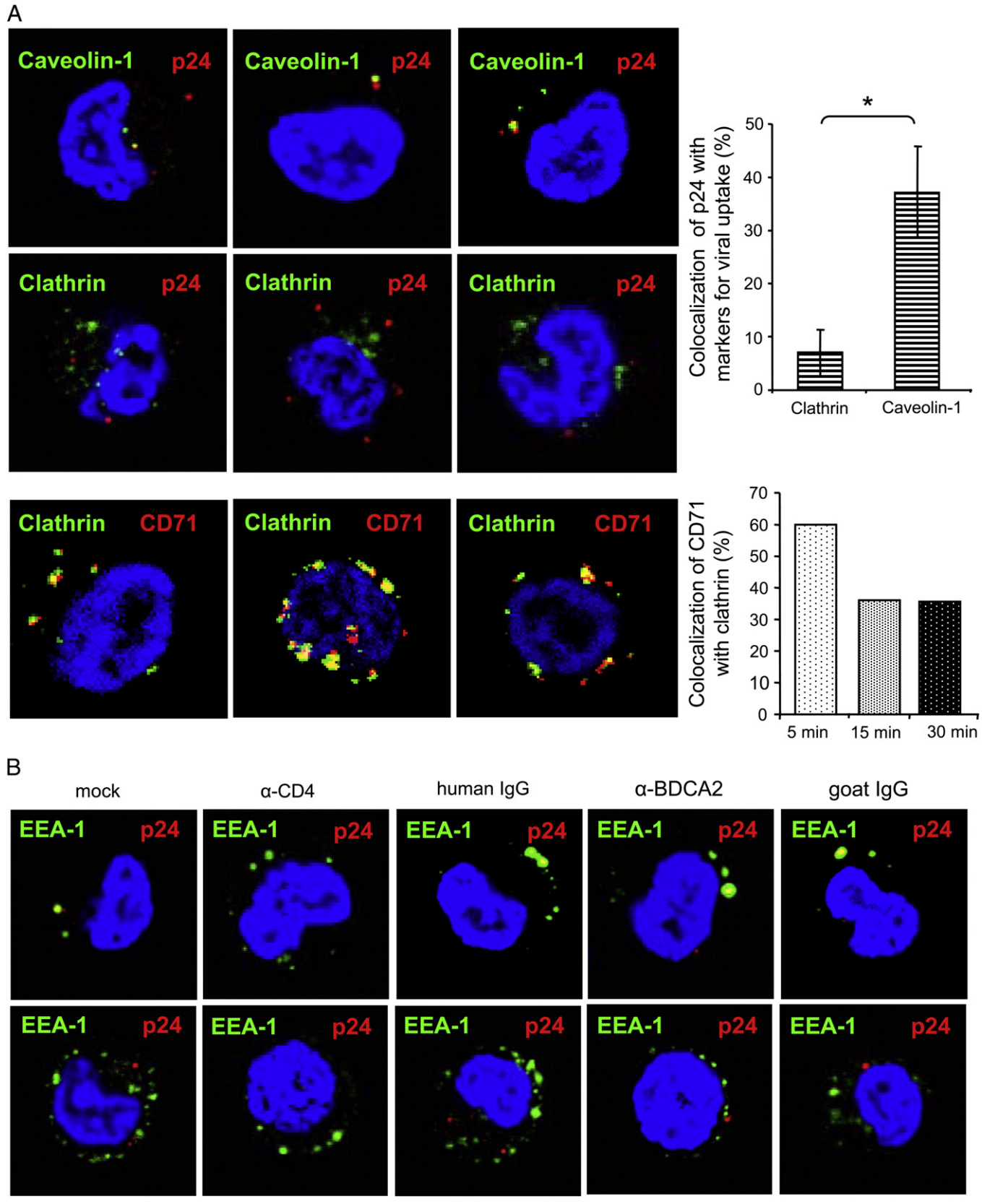

Fig. 7. Characterization of entry mechanism of HIV-1 into PDC. (A) PDC were exposed to HIV-1_{NL4-3} at 4 °C for 30 min and then incubated at 37 °C for different time periods. Cells were stained using a biotinylated antibody to the viral p24 capsid antigen (red) and monoclonal antibodies against clathrin or caveolin-1 (green). For quantification, double-positive cells were counted and the proportion of cells with a colocalization event was calculated. Cell nuclei were stained using DAPI (blue). Data represent three independent confocal experiments, evaluating a total of 111 and 152 double-positive cells for clathrin and caveolin-1, respectively. The results summarize all time points and are given as mean and standard error. *$p < 0.05$. As a control, HIV-1 exposed PDC of two different donors were stained with antibodies against clathrin (green) and CD71 (red). Results are representative for 172, 282, and 180 double-positive cells at 5, 15, and 30 min of incubation, respectively. (B) PDC were preincubated with mock (media), anti-CD4, human IgG (isotype for anti-CD4), anti-BDCA2, or goat IgG (isotype for BDCA2) for 2 h at 37 °C before they were exposed to HIV-1_{NL4-3} at 37 °C for 45 min. Cells were labeled with DAPI (blue), anti-p24 (red) and anti-EEA1 (green) and subsequently analyzed by confocal microscopy. The upper and lower panels show endosomal and cytosolic viral particles, respectively. The results are representative of two independent experiments.

intriguing evidence that cholesterol in the HIV-1 envelope was required to mediate IFN-alpha induction in PDC (Boasso et al., 2011).

The role of the CD4 receptor in the uptake of HIV-1 into PDC has been studied using antibodies against CD4, soluble CD4, and neutralizing antibodies to gp120, which blocked the HIV-1 induced IFN-alpha production (Beignon et al., 2005; Herbeuval et al., 2005a; Schmidt et al., 2005; Yonezawa et al., 2003). Correspondingly, changes in the gp120 protein that impaired CD4 binding and infectivity reduced the capacity of these viruses to induce IFN-alpha production (Haupt et al., 2008). An antibody to CD4 reduced the uptake of HIV-1 into PDC (Fig. 3E), although this effect was not as pronounced as in CD4+ T cells, suggesting that other factors are involved. More convincing were the blocking experiments, in which anti-CD4 inhibited the uptake of HIV-1 into cytosolic and endosomal compartments (Fig. 7B). These data confirm the crucial role of CD4 in the attachment and uptake of HIV-1 into PDC.

It remains unclear whether HIV-1 particles, viral capsids and/or nucleic acids can evade from the endosome into the cytosol and establish a productive infection, as reported for influenza viruses and others. HIV-1 was reported to establish productive infection in CD4+ HeLa cells after endocytosis (Daecke et al., 2005). Supporting evidence comes from studies reporting augmented HIV-1 infection after blocking lysosomal degradation (Fredericksen et al., 2002; Schaeffer et al., 2004; Wei et al., 2005). Myeloid dendritic cells can engulf viral particles and pass them on in an infectious form to CD4+ T cells (Cameron et al., 1992; Pope et al., 1994). This infection *in trans* is mediated by the C-type lectin DC-SIGN (Geijtenbeek et al., 2000). PDC can also transmit infectious viral particles to CD4+ T cells (Fong et al., 2002; Schmidt et al., 2004). However, the lack of colocalization with CD71 argues against this recycling mechanism in PDC (Fig. 6B).

The HIV-1 induced IFN-alpha production can be inhibited by blocking endosomal acidification (Beignon et al., 2005; Hardy et al., 2007; Schmidt et al., 2005; Lepelley et al., 2011). Hence, those particles which end up in the endosomes appear to be important for the IFN-alpha induction, supported by the colocalization of HIV-1 virions with late endosomal markers like Rab GTPases 7 and 9 and LAMP-1 (Figs. 5, 6). Subsequent release of viral nucleic acids may promote the interaction with the endosomal Toll-like receptors, as proposed by others (Beignon et al., 2005; Heil et al., 2004; Mandl et al., 2008; Lepelley et al., 2011). This concept may be physiologically relevant, because a very recent clinical study showed that the immune activation in 20 HIV-1 infected patients could be reduced by the administration of hydroxychloroquine (Piconi et al., 2011). Thus, our study provides new insights into the mechanisms by which PDC may contribute to the HIV-1 immunopathogenesis. These findings may encourage new therapeutic concepts that reduce the chronic immune activation in HIV-1 infection by inhibitors which interfere with the endocytic pathway.

Materials and methods

Isolation and cultivation of cells

PBMC were isolated from EDTA-anticoagulated blood of healthy volunteers using Ficoll density gradient centrifugation (Biochrom AG, Berlin, Germany), approved by the ethical committee of the Medical Faculty, Friedrich-Alexander Erlangen-Nürnberg (Ref. no. 3375). CD4+ T cells were purified from PBMC using a magnetic bead isolation kit (Miltenyi Biotech, Bergisch-Gladbach, Germany), and cultivated at a density of 3×10^6 cells/ml in RPMI 1640 (Gibco, Eggenstein, Germany) with 10% heat-inactivated (56 °C, 60 min) fetal calf serum (FCS) (Lonza, Basel, Switzerland), 50 mg/ml glutamine, 200 U/ml penicillin, and 90 U/ml streptomycin. Prior to HIV-1 infection, CD4+ T cells were stimulated with 1 μg/ml phytohemagglutinin (PHA) (Oxoid GmbH, Wesel, Germany) and 20 U/ml IL-2 (Roche Pharma, Reinach, Switzerland) for 3 days. PDC were isolated from PBMC using the BDCA4+ cell isolation kit (Miltenyi Biotech) (28). Cell viability was determined by trypan blue staining. The purity of isolated PDC, determined by CD4 and BDCA2 staining, was above 95%. PDC were plated at a density of $0.5–1\times10^6$ cells/ml in 24-well flat bottom plates unless indicated otherwise, and cultivated in the presence of 20 ng/ml IL-3 (R & D Systems, Wiesbaden-Nordenstadt, Germany). 293 T cells were cultivated in DMEM (Gibco) plus supplements.

Biologic reagents

The chimeric CD4 antibody (Leu3a) containing a murine Fab and a human Fc was kindly provided by Becton Dickinson, the p24 (71-31) antibody and the Trimeris/Roche fusion inhibitor T-20 (9845) by the NIH AIDS Research and Reference Reagent Program, Germantown, Maryland, and the TLR 7 agonist S-27609 by 3M Pharmaceuticals (St. Paul, MN). The cell-culture grade BDCA2 and isotype control antibody were obtained from R&D Systems (Wiesbaden-Nordenstadt, Germany), DMSO from AppliChem (Darmstadt, Germany), and dynasore (dissolved in DMSO) from Sigma-Aldrich (Taufkirchen, Germany).

Generation of virus stocks

PHA-stimulated CD4+ T cells were infected with the X4-tropic primary isolate HIV-1_{SF33} (Tateno and Levy, 1988). At peak viral replication, fluids were transferred to PHA-stimulated PBMC. Supernatants harvested at 3 days of infection were filtered through a 0.22 μM Millex-GS unit (Millipore, Schwalbach, Germany) and stored in aliquots. The tissue culture infectious dose 50% ($TCID_{50}$) was determined in PHA and IL-2 stimulated PBMC (McDougal et al., 1985). PDC were generally exposed to HIV-1_{SF33} at a multiplicity of infection (MOI) of 1. For HIV-1_{NL4-3} stocks, 293 T cells were plated in tissue culture dishes (Greiner Bio-one GmbH, Frickenhausen, Germany) and transfected at 80–90% confluency using FuGENE HD (Roche, Mannheim, Germany) (Haupt et al., 2008). Supernatants were ultracentrifuged through a 20% sucrose cushion (Beckmann SW41 rotor; 27,000 rpm, 90 min, 4 °C). An equivalent of 0.1–1 μg p24 antigen was used to infect 1×10^4 cells.

Quantification of virus

The abundance of HIV-1 RNA in the cellular fractionation experiments was quantified by the HIV-1 RealTime assay (Abbott, Wiesbaden-Delkenheim, Germany), and the amounts of p24 antigen by the Murex HIV antigen monoclonal antibody kit (Abbott).

Immuno-electron microscopy

Cells were exposed to HIV-1_{SF33} (MOI 1) or concentrated HIV-1_{NL4-3} at 37 °C for 60-90 min, fixed in 4% paraformaldehyde and 0.5% glutaraldehyde at room temperature (RT) for 90 min, incubated in 50 mM NH_4Cl for 10 min, and permeabilised in 0.2% Triton X-100 for 5 min. For pre-embedding immunostaining, a p24 antibody (71-31; 1:6) and a 12 nm Gold-conjugated anti-human IgG (Dianova, Hamburg, Germany; 1:20) were used. Cells were poststained with 1% osmium tetroxide for 60 min, dehydrated with ethanol/0.2% (wt/vol) uranyl acetate, and embedded in epon with propylenoxide. Polymerisation was performed at 60 °C for 3 days prior to sectioning with an Ultracut S microtome (Reichert-Jung). Sections were transferred to slot grids coated with Pioloform (Plano, Wetzlar, Germany), analyzed at a Technai™ G^2 electron microscope (FEI Company, Eindhoven, The Netherlands) at 120 kV, and recorded with a 2 K MegaView III digital camera (Olympus Software Imaging Solutions) at calibrated magnifications. For post-embedding immunostaining, cells fixed with 4% paraformaldehyde and 0.05% glutaraldehyde were dehydrated by graded alcohol, applying 0.5% uranylacetate with 30% ethanol to enhance section contrast, and embedded in Lowicryl (HM20) according to the progressive lowering temperature

technique. Thin sections applied to uncoated 400 Mesh nickel grids were incubated on droplets of blocking buffer (5% milk powder in DPBS) for 30 min, the p24 antibody (diluted 1:10 in DPBS with 0.5% BSA and 0.1% gelatine), and a 10 nm Gold-conjugated goat anti-human antibody (BBI, diluted 1:20 in PBS with 0.5% BSA and 0.1% gelatine) for 1 h. After fixation with 1% glutaraldehyde in 0.05% HEPES buffer, samples were counterstained with 2% uranyl acetate and lead citrate. Sections were examined using a TEM 902 (Carl Zeiss SMT AG, Germany) at 80 kV, and images were digitized using a slow-scan charge-coupled-device camera (Pro Scan; Scheuring, Germany).

Cellular fractionation

Cellular fractionation was performed as described by others (Janas et al., 2008; Marechal et al., 1998). A total of 1×10^6 cells were used for each condition. Since this quantity of PDC was not readily isolated from one donor, cells from 3 to 4 donors were pooled immediately prior to HIV-1 exposure. Cells were preincubated with anti-CD4 (15 μg/ml) for 2 h or the fusion inhibitor T-20 (100 nM, 300 nM, 500 nM and 1 μM) for 30 min before HIV-1_{SF33} was added. Cells were either incubated at 37 °C or kept on ice, then washed with ice-cold DPBS plus 0.1% FCS. All sedimentation steps were carried out at 4 °C in a pre-chilled centrifuge. To remove surface-bound HIV-1 particles, cells were treated with 0.25 mg/ml Pronase E (Sigma-Aldrich) in 20 mM HEPES buffer at 4 °C for 10 min, terminated by adding medium plus 10% FCS. Cells were washed twice using ice-cold DPBS plus 0.1% FCS and resuspended in 2 ml of swelling buffer (10 mM Tris–HCl, pH 8.0; 10 mM KCl; 1 mM EDTA). After incubation on ice for 15 min, cells were disrupted by 15 strokes of dounce homogenization. Debris and nuclear fractions were removed by centrifugation at 3000 rpm for 3 min. Supernatants were sedimented at 50,000 rpm for 13 min using a Beckman SW60Ti rotor to separate vesicles and cytosol. These conditions were validated using Jurkat T cells; supernatants of these cells were ultracentrifuged at 0–5–7–10–13–18–23–28 min and then analyzed using LAMP-1 Western blotting (data not shown). For further analysis, we adjusted the cytosolic fraction to 0.5% Triton X-100. The vesicular extract was lysed in a solution containing 20 mM HEPES, 0.5% Triton X-100, and 150 mM NaCl.

Western blot

Cytosolic and vesicular extracts of HIV-1 exposed PDC were prepared as described above. The vesicular pellet was resuspended in lysis buffer (50 mM TRIS, pH 8.0; 150 mM NaCl; 5 mM EDTA; 1% NP-40; 0.1 mM PMSF). The volume of the cytosolic fraction was adjusted to the vesicular fraction using Amicon Ultra-4 Centrifugal Filter Units with Ultracel-30 membrane (Millipore). The SDS-denatured samples were separated on a 10% polyacrylamide gel, transferred to a PVDF membrane (Millipore), and blocked with 5% milk powder. The LAMP-1 antibody (Natutec, Frankfurt, Germany; 1:500) was incubated at 4 °C overnight and a HRP-conjugated rabbit polyclonal anti-mouse IgG (H + L) (DAKO Diagnostics GmbH, Hamburg; 1:1000) at RT for 90 min. After addition of ECL solution containing luminol (Sigma) for 1 min, luminescence was documented using the Fujifilm LAS-1000 plus gel documentation system.

IFN-alpha assays

PDC were plated at 1×10^4 cells in 96-well plates, pretreated with T-20 (100 and 300 nM), and stimulated with UV-inactivated herpes simplex virus type 1 (HSV-1) at 1×10^6 PFU/ml (Schuster et al., 2010) or HIV-1_{NL4-3}. In other experiments, PDC were preincubated with dynasore (80 μM) or equivalent volumes of DMSO, and exposed to S-27609 (5 μM) or HIV-1_{NL4-3}. In some experiments, PDC were incubated with dynasore and HIV-1 in serum-free media; after 2 h, FCS was added. Supernatants were harvested after 36 h and IFN-alpha production was analyzed using an ELISA module set (Bender MedSystems, Vienna, Austria).

Confocal microscopy

PDC were cultivated in IL-3 containing medium overnight before they were incubated with HIV-1_{SF33} or HIV-1_{NL4-3} at 4 °C for 30–60 min and then at 37 °C for different time periods. Cells were washed once in cold DPBS, transferred to glass slides (Medco Diagnostika GmbH, Munich, Germany), and fixed with 4% PFA for 1 h. Slides were washed three times in DPBS plus 0.05% Tween 20, blocked and permeabilised in DPBS with 1% BSA and 0.02% saponin for 30 min. The biotinylated goat anti-p24 antibody (1:100) (ViroStat, Portland, ME) was incubated at 4 °C overnight together with the respective primary antibodies, the murine antibodies against LAMP-1 (see above; 1:100), CD71 (Acris Antibodies, Herford, Germany; 1:100), CD63 (1:1000) and CD81 (1:1000) (BD Biosciences, Heidelberg, Germany), or rabbit antibodies against EEA-1 (1:100), the Rab GTPases 5 (1:100), 7 (1:50), and 9 (1:100), Clathrin (1:50), and Caveolin-1 (1:400) (Cell Signaling, distributed by New England Biolabs, Frankfurt, Germany). Mouse IgG1 (Immunotools, Friesoythe, Germany) and rabbit IgG (Cell Signaling) served as isotype controls. After three washing steps, slides were incubated with an Alexa Fluor 488-conjugated goat F(ab′)2 fragment anti-mouse IgG (H + L) antibody (1:1000) or an Alexa Fluor 488-conjugated goat F(ab′)2 fragment anti-rabbit IgG (H + L) (1:500) (both Invitrogen, Karlsruhe, Germany), and Streptavidin-TRITC (1:75) (Serotec, Düsseldorf, Germany) at RT for 90 min. DAPI (300 nM) was added 5 min prior to mounting the coverslips using Fluoprep (Biomérieux, Nürtingen, Germany) or Vectashield (Biozol, Eiching, Germany). Cells were analyzed using the TCS SP5 laser scanning microscope equipped with the LAS-AF software (Leica Microsystems, Mannheim, Germany). To quantify the colocalization of the viral capsid protein p24 with cellular markers, double-labeled cells were counted and the proportion of cells with a colocalization event was calculated. Movies were obtained using the Leica Visualization 3D-Projection program. For the blocking experiments, PDC were preincubated with the antibodies to CD4 or BDCA2 (7.5–15 μg/ml) or the respective isotype controls for 2 h at 37 °C prior to HIV-1 exposure. Confocal staining was performed as described above.

Statistics

The abundance of HIV-1 RNA in different cell fractions, IFN-alpha values, and colocalization events were compared using the Student's t-tests for paired and unpaired samples. Two-sided p values <0.05 were considered significant.

Supplementary data to this article can be found online at doi:10.1016/j.virol.2011.11.026.

Acknowledgments

We thank Jay A. Levy for kindly providing the primary X4-tropic HIV-1_{SF33} isolate, Becton Dickinson for the chimeric CD4 antibody Leu3a, and 3M Pharmaceuticals for S-27609. We want to acknowledge funding by the German Research Foundation (SCHM1702/2-1; SCHM1702/2-2; SCHM1702/3-1), the German Competence Network for HIV/AIDS, the "Gesellschaft für AIDS-Forschung", and the "Akademie der Wissenschaften und Literatur zu Mainz". Philipp Schuster and Sabrina Haupt were supported by the graduate college 1071 ("Viruses of the immune system"; Project B5), and Moritz Ries by the IZKF Erlangen (TR50). Elke Bogner's part of the research was supported by the German Research Foundation (Bo 1214/15-1) and the Wilhelm Sander Foundation (No. 2004.031.2).

References

Beignon, A.S., McKenna, K., Skoberne, M., Manches, O., Dasilva, I., Kavanagh, D.G., Larsson, M., Gorelick, R.J., Lifson, J.D., Bhardwaj, N., 2005. Endocytosis of HIV-1 activates plasmacytoid dendritic cells via Toll-like receptor-viral RNA interactions. J. Clin. Invest. 115, 3265–3275.

Bennett, A.E., Narayan, K., Shi, D., Hartnell, L.M., Gousset, K., He, H., Lowekamp, B.C., Yoo, T.S., Bliss, D., Freed, E.O., Subramaniam, S., 2009. Ion-abrasion scanning electron microscopy reveals surface-connected tubular conduits in HIV-infected macrophages. PLoS Pathog. 5, e1000591.

Blanco, J., Bosch, B., Fernandez-Figueras, M.T., Barretina, J., Clotet, B., Este, J.A., 2004. High level of coreceptor-independent HIV transfer induced by contacts between primary CD4 T cells. J. Biol. Chem. 279, 51305–51314.

Boasso, A., Royle, C.M., Doumazos, S., Aquino, V.N., Biasin, M., Piacentini, L., Tavano, B., Fuchs, D., Mazzotta, F., Lo, C.S., Shearer, G.M., Clerici, M., Graham, D.R., 2011. Overactivation of plasmacytoid dendritic cells inhibits antiviral T-cell responses: a model for HIV immunopathogenesis. Blood 118, 5152–5162.

Cameron, P.U., Freudenthal, P.S., Barker, J.M., Gezelter, S., Inaba, K., Steinman, R.M., 1992. Dendritic cells exposed to human immunodeficiency virus type-1 transmit a vigorous cytopathic infection to CD4+ T cells. Science 257, 383–387.

Carter, G.C., Bernstone, L., Baskaran, D., James, W., 2011. HIV-1 infects macrophages by exploiting an endocytic route dependent on dynamin, Rac1 and Pak1. Virology 409, 234–250.

Cella, M., Jarrossay, D., Facchetti, F., Alebardi, O., Nakajima, H., Lanzavecchia, A., Colonna, M., 1999. Plasmacytoid monocytes migrate to inflamed lymph nodes and produce large amounts of type I interferon. Nat. Med. 5, 919–923.

Cella, M., Facchetti, F., Lanzavecchia, A., Colonna, M., 2000. Plasmacytoid dendritic cells activated by influenza virus and CD40L drive a potent TH1 polarization. Nat. Immunol. 1, 305–310.

Daecke, J., Fackler, O.T., Dittmar, M.T., Krausslich, H.G., 2005. Involvement of clathrin-mediated endocytosis in human immunodeficiency virus type 1 entry. J. Virol. 79, 1581–1594.

Di Pucchio, T., Chatterjee, B., Smed-Sorensen, A., Clayton, S., Palazzo, A., Montes, M., Xue, Y., Mellman, I., Banchereau, J., Connolly, J.E., 2008. Direct proteasome-independent cross-presentation of viral antigen by plasmacytoid dendritic cells on major histocompatibility complex class I. Nat. Immunol. 9, 551–557.

Dzionek, A., Sohma, Y., Nagafune, J., Cella, M., Colonna, M., Facchetti, F., Gunther, G., Johnston, I., Lanzavecchia, A., Nagasaka, T., Okada, T., Vermi, W., Winkels, G., Yamamoto, T., Zysk, M., Yamaguchi, Y., Schmitz, J., 2001. BDCA-2, a novel plasmacytoid dendritic cell-specific type II C-type lectin, mediates antigen capture and is a potent inhibitor of interferon alpha/beta induction. J. Exp. Med. 194, 1823–1834.

Ehrlich, M., Boll, W., Van, O.A., Hariharan, R., Chandran, K., Nibert, M.L., Kirchhausen, T., 2004. Endocytosis by random initiation and stabilization of clathrin-coated pits. Cell 118, 591–605.

Fitzgerald-Bocarsly, P., Feng, D., 2007. The role of type I interferon production by dendritic cells in host defense. Biochimie 89, 843–855.

Fitzgerald-Bocarsly, P., Jacobs, E.S., 2010. Plasmacytoid dendritic cells in HIV infection: striking a delicate balance. J. Leukoc. Biol. 87, 609–620.

Fong, L., Mengozzi, M., Abbey, N.W., Herndier, B.G., Engleman, E.G., 2002. Productive infection of plasmacytoid dendritic cells with human immunodeficiency virus type 1 is triggered by CD40 ligation. J. Virol. 76, 11033–11041.

Fonteneau, J.F., Larsson, M., Beignon, A.S., McKenna, K., Dasilva, I., Amara, A., Liu, Y.J., Lifson, J.D., Littman, D.R., Bhardwaj, N., 2004. Human immunodeficiency virus type 1 activates plasmacytoid dendritic cells and concomitantly induces the bystander maturation of myeloid dendritic cells. J. Virol. 78, 5223–5232.

Fredericksen, B.L., Wei, B.L., Yao, J., Luo, T., Garcia, J.V., 2002. Inhibition of endosomal/lysosomal degradation increases the infectivity of human immunodeficiency virus. J. Virol. 76, 11440–11446.

Geijtenbeek, T.B., Kwon, D.S., Torensma, R., van Vliet, S.J., van Duijnhoven, G.C., Middel, J., Cornelissen, I.L., Nottet, H.S., KewalRamani, V.N., Littman, D.R., Figdor, C.G., van, K.Y., 2000. DC-SIGN, a dendritic cell-specific HIV-1-binding protein that enhances trans-infection of T cells. Cell 100, 587–597.

Gilliet, M., Cao, W., Liu, Y.J., 2008. Plasmacytoid dendritic cells: sensing nucleic acids in viral infection and autoimmune diseases. Nat. Rev. Immunol. 8, 594–606.

Giorgi, J.V., Hultin, L.E., McKeating, J.A., Johnson, T.D., Owens, B., Jacobson, L.P., Shih, R., Lewis, J., Wiley, D.J., Phair, J.P., Wolinsky, S.M., Detels, R., 1999. Shorter survival in advanced human immunodeficiency virus type 1 infection is more closely associated with T lymphocyte activation than with plasma virus burden or virus chemokine coreceptor usage. J. Infect. Dis. 179, 859–870.

Hanover, J.A., Willingham, M.C., Pastan, I., 1984. Kinetics of transit of transferrin and epidermal growth factor through clathrin-coated membranes. Cell 39, 283–293.

Hardy, A.W., Graham, D.R., Shearer, G.M., Herbeuval, J.P., 2007. HIV turns plasmacytoid dendritic cells (pDC) into TRAIL-expressing killer pDC and down-regulates HIV coreceptors by Toll-like receptor 7-induced IFN-alpha. Proc. Natl. Acad. Sci. U. S. A. 104, 17453–17458.

Haupt, S., Donhauser, N., Chaipan, C., Schuster, P., Puffer, B., Daniels, R.S., Greenough, T.C., Kirchhoff, F., Schmidt, B., 2008. CD4 binding affinity determines human immunodeficiency virus type 1-induced alpha interferon production in plasmacytoid dendritic cells. J. Virol. 82, 8900–8905.

Heil, F., Hemmi, H., Hochrein, H., Ampenberger, F., Kirschning, C., Akira, S., Lipford, G., Wagner, H., Bauer, S., 2004. Species-specific recognition of single-stranded RNA via toll-like receptor 7 and 8. Science 303, 1526–1529.

Herbeuval, J.P., Grivel, J.C., Boasso, A., Hardy, A.W., Chougnet, C., Dolan, M.J., Yagita, H., Lifson, J.D., Shearer, G.M., 2005a. CD4+ T-cell death induced by infectious and non-infectious HIV-1: role of type 1 interferon-dependent, TRAIL/DR5-mediated apoptosis. Blood 106, 3524–3531.

Herbeuval, J.P., Hardy, A.W., Boasso, A., Anderson, S.A., Dolan, M.J., Dy, M., Shearer, G.M., 2005b. Regulation of TNF-related apoptosis-inducing ligand on primary CD4+ T cells by HIV-1: role of type I IFN-producing plasmacytoid dendritic cells. Proc. Natl. Acad. Sci. U. S. A. 102, 13974–13979.

Herbeuval, J.P., Nilsson, J., Boasso, A., Hardy, A.W., Kruhlak, M.J., Anderson, S.A., Dolan, M.J., Dy, M., Andersson, J., Shearer, G.M., 2006. Differential expression of IFN-alpha and TRAIL/DR5 in lymphoid tissue of progressor versus nonprogressor HIV-1-infected patients. Proc. Natl. Acad. Sci. U. S. A. 103, 7000–7005.

Janas, A.M., Dong, C., Wang, J.H., Wu, L., 2008. Productive infection of human immunodeficiency virus type 1 in dendritic cells requires fusion-mediated viral entry. Virology 375, 442–451.

Kadowaki, N., Antonenko, S., Lau, J.Y.N., Liu, Y.J., 2000. Natural interferon alpha/beta-producing cells link innate and adaptive immunity. J. Exp. Med. 192, 219–225.

Kilby, J.M., Hopkins, S., Venetta, T.M., DiMassimo, B., Cloud, G.A., Lee, J.Y., Alldredge, L., Hunter, E., Lambert, D., Bolognesi, D., Matthews, T., Johnson, M.R., Nowak, M.A., Shaw, G.M., Saag, M.S., 1998. Potent suppression of HIV-1 replication in humans by T-20, a peptide inhibitor of gp41-mediated virus entry. Nat. Med. 4, 1302–1307.

Kirchhoff, F., 2009. Is the high virulence of HIV-1 an unfortunate coincidence of primate lentiviral evolution? Nat. Rev. Microbiol. 7, 467–476.

Lee, H.K., Lund, J.M., Ramanathan, B., Mizushima, N., Iwasaki, A., 2007. Autophagy-dependent viral recognition by plasmacytoid dendritic cells. Science 315, 1398–1401.

Lepelley, A., Louis, S., Sourisseau, M., Law, H.K., Pothlichet, J., Schilte, C., Chaperot, L., Plumas, J., Randall, R.E., Si-Tahar, M., Mammano, F., Albert, M.L., Schwartz, O., 2011. Innate sensing of HIV-infected cells. PLoS Pathog. 7, e1001284.

Macia, E., Ehrlich, M., Massol, R., Boucrot, E., Brunner, C., Kirchhausen, T., 2006. Dynasore, a cell-permeable inhibitor of dynamin. Dev. Cell 10, 839–850.

Mandl, J.N., Barry, A.P., Vanderford, T.H., Kozyr, N., Chavan, R., Klucking, S., Barrat, F.J., Coffman, R.L., Staprans, S.I., Feinberg, M.B., 2008. Divergent TLR7 and TLR9 signaling and type I interferon production distinguish pathogenic and nonpathogenic AIDS virus infections. Nat. Med. 14, 1077–1087.

Marechal, V., Clavel, F., Heard, J.M., Schwartz, O., 1998. Cytosolic Gag p24 as an index of productive entry of human immunodeficiency virus type 1. J. Virol. 72, 2208–2212.

Marechal, V., Prevost, M.C., Petit, C., Perret, E., Heard, J.M., Schwartz, O., 2001. Human immunodeficiency virus type 1 entry into macrophages mediated by macropinocytosis. J. Virol. 75, 11166–11177.

Martin, F., Roth, D.M., Jans, D.A., Pouton, C.W., Partridge, L.J., Monk, P.N., Moseley, G.W., 2005. Tetraspanins in viral infections: a fundamental role in viral biology? J. Virol. 79, 10839–10851.

Martinelli, E., Cicala, C., Van Ryk, D., Goode, D.J., Macleod, K., Arthos, J., Fauci, A.S., 2007. HIV-1 gp120 inhibits TLR9-mediated activation and IFN-{alpha} secretion in plasmacytoid dendritic cells. Proc. Natl. Acad. Sci. U. S. A. 104, 3396–3401.

Martinson, J.A., Montoya, C.J., Usuga, X., Ronquillo, R., Landay, A.L., Desai, S.N., 2010. Chloroquine modulates HIV-1-induced plasmacytoid dendritic cell alpha interferon: implication for T-cell activation. Antimicrob. Agents Chemother. 54, 871–881.

McDougal, J.S., Cort, S.P., Kennedy, M.S., Cabridilla, C.D., Feorino, P.M., Francis, D.P., Hicks, D., Kalyanaraman, V.S., Martin, L.S., 1985. Immunoassay for the detection and quantitation of infectious human retrovirus, lymphadenopathy-associated virus (LAV). J. Immunol. Methods 76, 171–183.

Mercer, J., Schelhaas, M., Helenius, A., 2010. Virus entry by endocytosis. Annu. Rev. Biochem. 79, 803–833.

Meythaler, M., Martinot, A., Wang, Z., Pryputniewicz, S., Kasheta, M., Ling, B., Marx, P.A., O'Neil, S., Kaur, A., 2009. Differential CD4+ T-lymphocyte apoptosis and bystander T-cell activation in rhesus macaques and sooty mangabeys during acute simian immunodeficiency virus infection. J. Virol. 83, 572–583.

Miyauchi, K., Kim, Y., Latinovic, O., Morozov, V., Melikyan, G.B., 2009. HIV enters cells via endocytosis and dynamin-dependent fusion with endosomes. Cell 137, 433–444.

Mu, F.T., Callaghan, J.M., Steele-Mortimer, O., Stenmark, H., Parton, R.G., Campbell, P.L., McCluskey, J., Yeo, J.P., Tock, E.P., Toh, B.H., 1995. EEA1, an early endosome-associated protein. EEA1 is a conserved alpha-helical peripheral membrane protein flanked by cysteine "fingers" and contains a calmodulin-binding IQ motif. J. Biol. Chem. 270, 13503–13511.

O'Brien, M., Manches, O., Sabado, R.L., Baranda, S.J., Wang, Y., Marie, I., Rolnitzky, L., Markowitz, M., Margolis, D.M., Levy, D., Bhardwaj, N., 2011. Spatiotemporal trafficking of HIV in human plasmacytoid dendritic cells defines a persistently IFN-alpha-producing and partially matured phenotype. J. Clin. Invest. 121, 1088–1101.

Permanyer, M., Ballana, E., Este, J.A., 2010. Endocytosis of HIV: anything goes. Trends Microbiol. 18, 543–551.

Piconi, S., Parisotto, S., Rizzardini, G., Passerini, S., Terzi, R., Argenteri, B., Meraviglia, P., Capetti, A., Biasin, M., Trabattoni, D., Clerici, M., 2011. Hydroxychloroquine drastically reduces immune activation in HIV-infected, ART-treated, immunological non-responders. Blood 118, 3263–3272.

Pope, M., Betjes, M.G., Romani, N., Hirmand, H., Cameron, P.U., Hoffman, L., Gezelter, S., Schuler, G., Steinman, R.M., 1994. Conjugates of dendritic cells and memory T lymphocytes from skin facilitate productive infection with HIV-1. Cell 78, 389–398.

Rubino, M., Miaczynska, M., Lippe, R., Zerial, M., 2000. Selective membrane recruitment of EEA1 suggests a role in directional transport of clathrin-coated vesicles to early endosomes. J. Biol. Chem. 275, 3745–3748.

Schaeffer, E., Soros, V.B., Greene, W.C., 2004. Compensatory link between fusion and endocytosis of human immunodeficiency virus type 1 in human CD4 T lymphocytes. J. Virol. 78, 1375–1383.

Schelhaas, M., 2010. Come in and take your coat off—how host cells provide endocytosis for virus entry. Cell. Microbiol. 12, 1378–1388.

Schmidt, B., Scott, I., Whitmore, R.G., Foster, H., Fujimura, S., Schmitz, J., Levy, J.A., 2004. Low-level HIV infection of plasmacytoid dendritic cells: onset of cytopathic effects and cell death after PDC maturation. Virology 329, 280–288.

Schmidt, B., Ashlock, B.M., Foster, H., Fujimura, S.H., Levy, J.A., 2005. HIV-infected cells are major inducers of plasmacytoid dendritic cell interferon production, maturation, and migration. Virology 343, 256–266.

Schuster, P., Donhauser, N., Pritschet, K., Ries, M., Haupt, S., Kittan, N.A., Korn, K., Schmidt, B., 2010. Co-ordinated regulation of plasmacytoid dendritic cell surface receptors upon stimulation with herpes simplex virus type 1. Immunology 129, 234–247.

Siegal, F.P., Kadowaki, N., Shodell, M., Fitzgerald-Bocarsly, P.A., Shah, K., Ho, S., Antonenko, S., Liu, Y.J., 1999. The nature of the principal type 1 interferon-producing cells in human blood. Science 284, 1835–1837.

Sousa, A.E., Carneiro, J., Meier-Schellersheim, M., Grossman, Z., Victorino, R.M., 2002. CD4 T cell depletion is linked directly to immune activation in the pathogenesis of HIV-1 and HIV-2 but only indirectly to the viral load. J. Immunol. 169, 3400–3406.

Tateno, M., Levy, J.A., 1988. MT-4 plaque formation can distinguish cytopathic subtypes of the human immunodeficiency virus (HIV). Virology 167, 299–301.

van Spriel, A.B., Figdor, C.G., 2010. The role of tetraspanins in the pathogenesis of infectious diseases. Microbes Infect. 12, 106–112.

Wei, B.L., Denton, P.W., O'Neill, E., Luo, T., Foster, J.L., Garcia, J.V., 2005. Inhibition of lysosome and proteasome function enhances human immunodeficiency virus type 1 infection. J. Virol. 79, 5705–5712.

Yonezawa, A., Morita, R., Takaori-Kondo, A., Kadowaki, N., Kitawaki, T., Hori, T., Uchiyama, T., 2003. Natural alpha interferon-producing cells respond to human immunodeficiency virus type 1 with alpha interferon production and maturation into dendritic cells. J. Virol. 77, 3777–3784.